

# Charge Polarization at a Au-TiC Interface and the Generation of Highly Active and Selective Catalysts for the Low-Temperature Water Gas Shift Reaction.

José A Rodríguez,<sup>[a]</sup> Pedro J. Ramirez,<sup>[a,b]</sup> Gian Giacomo Asara,<sup>[c,d]</sup> Francesc Viñes,<sup>[d]</sup> Jaime Evans,<sup>[b]</sup> Ping Liu,<sup>[a]</sup> Josep M. Ricart,<sup>[c]</sup> and Francesc Illas<sup>[d]</sup>

Transition metal nanoparticles dispersed on oxides or carbon supports are among the most frequently used catalysts in the chemical and petrochemical industries. In principle, by selecting the right combination of metal and support, one could reduce substantially the energy necessary for chemical transformations and optimize the use of chemical feedstocks.<sup>[1]</sup> Metal-support interactions can have negative<sup>[2,3]</sup> or positive<sup>[4,5]</sup> effects on the catalytic properties of a metal. A major challenge in heterogeneous catalysis is to understand metal-support interactions at an atomic level and use them to design highly active and selective catalysts.<sup>[1,4,5]</sup> In the last decades, a large effort has been focused on the study of metal-oxide interactions.<sup>[1]</sup> However, in recent years, it has become clear that metal carbides can be excellent supports for the dispersion of metal catalysts.<sup>[6-10]</sup> The metal carbides have interesting catalytic properties on their own,<sup>[11-18]</sup> and they also can modify the reactivity of a supported metal through chemical bonding.<sup>[8,19]</sup> In this article we investigate the performance of Au/TiC(001) surfaces as catalysts for the water-gas shift reaction ( $\text{CO} + \text{H}_2\text{O} \rightarrow \text{H}_2 + \text{CO}_2$ , WGS). The WGS is a key process in the industrial production of hydrogen.<sup>[20,21]</sup> Commercial catalysts for the WGS usually involve mixtures Fe-Cr and Cu-Zn oxides, used at temperatures between 620-770 K and 470-525 K, respectively.<sup>[20]</sup> These catalysts normally require lengthy and complex activation steps before usage. There is a general desire to find WGS catalysts active at relatively low temperatures ( $< 470$  K).<sup>[20]</sup> Metal-carbide based catalysts can accomplish this task,<sup>[6,14,17,18]</sup> but there are serious concerns about their stability and selectivity.<sup>[14,18]</sup> Many metal carbides are sensitive to  $\text{O}_2$  or

O-containing molecules in the reaction feed.<sup>[11,14,18]</sup> On the other hand, metal carbides can be very active for the breaking of the C-O bond in carbon monoxide<sup>[11,22]</sup> and, in the presence of hydrogen, hydrogenate the produced C atoms to yield methane or higher alkanes.<sup>[10,13,15,16,23]</sup> Our study indicates that the 1:1 metal-to-carbon ratio in TiC gives stability to this carbide substrate and prevents the cleavage of C-O bonds. Strong metal-support interactions make Au/TiC(001) a highly active and selective catalyst for the low-temperature WGS reaction.

Figure 1 shows the WGS activity for clean TiC(001) and Au/TiC(001) surfaces as a function of Au coverage. We found that the clean TiC(001) surface is able to catalyze the WGS, in agreement with the predictions of previous DFT calculations.<sup>[17]</sup> In fact, at 450 K, TiC(001) displays a WGS activity larger than that of Cu(111),<sup>[24]</sup> a typical benchmark in WGS studies.<sup>[21,24]</sup> Metallic Au does not catalyze the WGS.<sup>[26]</sup> In spite of this, the addition of Au to TiC(001) produces a drastic increase in the WGS activity of the system. A maximum in the production of  $\text{H}_2$  and  $\text{CO}_2$  is observed at  $\theta_{\text{Au}} \sim 0.15$  ML. After this point, there is a gradual decrease in the WGS activity of Au/TiC(001). Studies of STM have shown that at coverages below 0.2 ML, Au grows on TiC(001) forming a large amount of two dimensional (2D) particles.<sup>[8,19]</sup> The Au atoms in this 2D particles are in direct contact with the C sites of the TiC(001) substrate undergoing a charge polarization<sup>[25]</sup> which enhances their chemical reactivity.<sup>[8,9,19]</sup> At Au coverages above 0.2 ML, the admetal forms predominantly three-dimensional (3D) particles (i.e. the Au

- [a] Dr J.A. Rodríguez, Dr P.J. Ramirez, Dr P. Liu  
Chemistry Department, Brookhaven National Laboratory  
Upton, NY 11973 (USA)  
E-mail: rodriguez@bnl.gov
- [b] Dr P.J. Ramirez, Prof J. Evans  
Facultad de Ciencias, Universidad Central de Venezuela  
Caracas 1020A (Venezuela)
- [c] G.-G. Asara, Prof J.M. Ricart  
Departament de Química Física i Inorgànica, Universitat Rovira i Virgili, C/ Marcel·lí Domingo s/n, 43007 Tarragona (Spain)
- [d] G.-G. Asara, Dr F. Viñes, Prof F. Illas  
Departament de Química Física i IQTCUB, Universitat de Barcelona, C/Martí i Franquès 1, 08028 Barcelona (Spain)
- [\*\*] The work at BNL was financed by the US Department of Energy (DOE), Office of Basic Energy Science (DE-AC02-98CH10086). This work has been supported by the Spanish MINECO grant CTQ2012-30751 grant and, in part, by Generalitat de Catalunya grants 2014SGR97 and XRQTC. INTEVEP and IDB financed the work done at UCV. G.-G. A thanks the *Universitat Rovira i Virgili* for supporting his predoctoral research. F.V. thanks the MINECO for a postdoctoral *Ramón y Cajal* grant (RYC-2012-10129). F.I. acknowledges additional support through the ICREA Academic award for excellence in research. Computational time at the MARENOSTRUM supercomputer has been generously provided by the Barcelona Supercomputer Centre through a grant from *Red Española de Supercomputación*.

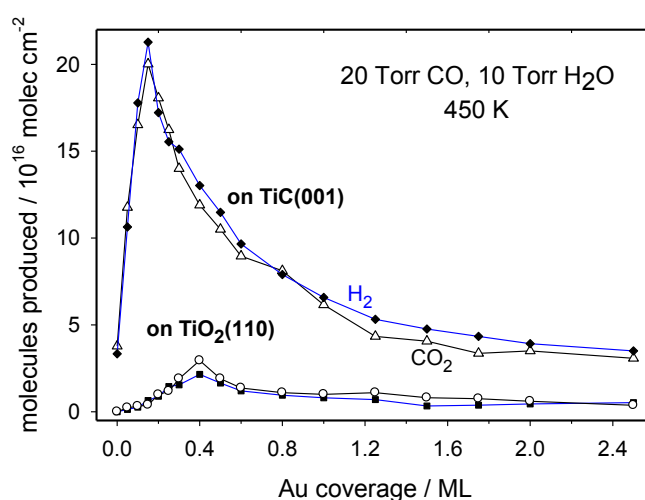


**Figure 1.** WGS activity of Au/TiC(001) and Au/TiO<sub>2</sub>(110) as a function of Au coverage. The reported values for the production of  $\text{H}_2$  (filled symbols) and  $\text{CO}_2$  (empty symbols) were obtained after exposing the catalysts to 20 Torr of CO and 10 Torr of  $\text{H}_2\text{O}$  at 450 K for 5 min.

atoms exposed to the reactants are not electronically modified by interactions with the carbide support) and the chemical reactivity of the system decreases.<sup>[8,19]</sup>

In Figure 1, we compare the WGS activity of a series of Au/TiC(001) and Au/TiO<sub>2</sub>(110) surfaces with similar coverages of the admetal. At temperatures of 550-625 K, Au/TiO<sub>2</sub> is known to be a very good catalyst for the WGS<sup>[26]</sup> with an activity that is higher than that of Cu/ZnO<sup>[27]</sup> which is used as an industrial WGS catalyst.<sup>[20]</sup> The results in Figure 1 indicate that Au/TiC(001) is a much better low-temperature WGS catalysts than Au/TiO<sub>2</sub>(110). This is corroborated by the data shown in the Arrhenius plots of Figure 2. The apparent activation energy for the WGS process decreases from 18 kcal/mol on Cu(111) to 10 kcal/mol on Au/TiO<sub>2</sub>(110) and 8 kcal/mol on Au/TiC(001). At relatively low temperatures (< 470 K), Au/TiC(001) exhibits a WGS activity that is observed on copper surfaces and on Cu/oxide or Au/oxide (oxide= TiO<sub>2</sub>, ZnO, CeO<sub>2</sub>, MgO) catalysts only at elevated temperatures (> 500 K).<sup>[26,27]</sup>

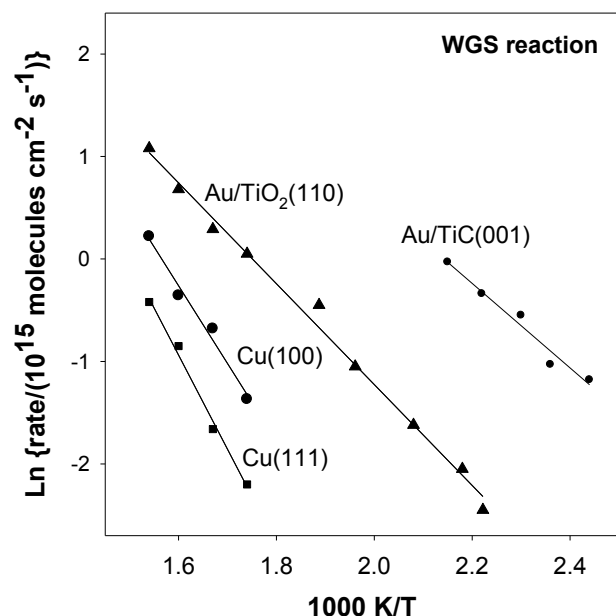


**Figure 2.** Arrhenius plots for the WGS on Cu(111), Cu(100), Au/TiO<sub>2</sub>(110) and Au/TiC(001) catalysts (20 Torr of CO and 10 Torr of H<sub>2</sub>O). Surfaces of metallic Au are not active for the WGS reaction. The data for Cu(111), Cu(100), Cu(111) and Au/TiO<sub>2</sub>(110) were taken from refs. [26,27]. The coverages of Au on TiO<sub>2</sub>(110) and TiC(001) were 0.4 and 0.15 ML, respectively. At these coverages maximum catalytic activity was observed for Au/TiO<sub>2</sub>(110) and Au/TiC(001).

From the data points in Figure 2, we estimated turnover frequencies (TOFs) for Au/TiC(001) assuming that all the gold atoms in the catalyst were involved in the WGS process. This is a valid assumption since STM shows that at a low coverage of Au (~ 0.15 ML) the admetal grows forming a substantial amount of 2D islands on TiC(001).<sup>[8,19]</sup> The estimated TOFs at different temperatures are shown in the top panel in Figure 3. The bottom panel compares TOFs for several catalysts. Again it is clear that

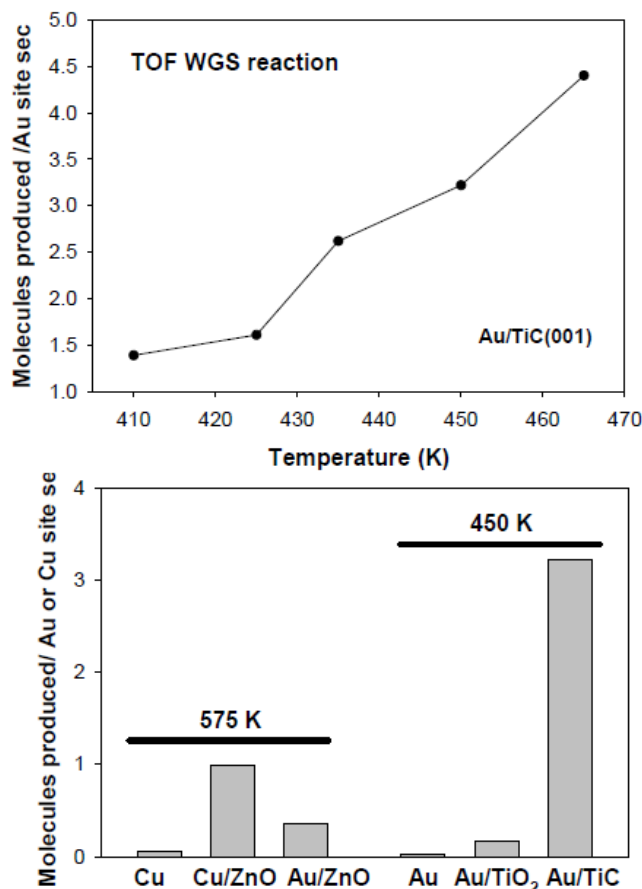


**Figure 3.** Top: TOFs for the WGS reaction on Au/TiC(001) at different temperatures. Bottom: Comparison of the TOFs for the WGS on Cu(111)<sup>[26]</sup>, Cu/ZnO(000T)<sup>[27]</sup>, Au/ZnO(000T)<sup>[27]</sup>, Au(111)<sup>[26]</sup>, Au/TiO<sub>2</sub>(110)<sup>[26]</sup> and Au/TiC(001). In all cases, the pressures of CO and H<sub>2</sub>O were 20 and 10 Torr, respectively.

Au/TiC(001) is an excellent catalyst for the WGS reaction. A Cu/ZnO(000T) surface, which models industrial Cu/ZnO catalysts,<sup>[27]</sup> displays a TOF ~ 3 times smaller than that of Au/TiC(001) in spite of an increase of 125 K in the reaction temperature.

As mentioned above, two important issues when dealing with the use of metal carbides as possible catalysts for the WGS are selectivity and stability.<sup>[14-18]</sup> In many industrial operations, the WGS is performed under hydrogen rich conditions with mixtures of CO/H<sub>2</sub>O/H<sub>2</sub> that come from the reforming of hydrocarbons.<sup>[6,14]</sup> Under hydrogen rich conditions metal carbides such as Mo<sub>2</sub>C transform CO into methane as a side reaction.<sup>[15,22]</sup> We performed studies comparing the WGS process on Au/TiC(001) and Au/Mo<sub>2</sub>C(001) using CO/H<sub>2</sub>O/H<sub>2</sub> mixtures. A gold coverage of ~ 0.15 ML was deposited on TiC(001) and on a Mo<sub>2</sub>C(001) surface.<sup>[13]</sup> The results are summarized in Figure 4. Neither TiC(001) nor Au/TiC(001) produce methane as a reaction product. These catalysts only produce CO<sub>2</sub> through the WGS

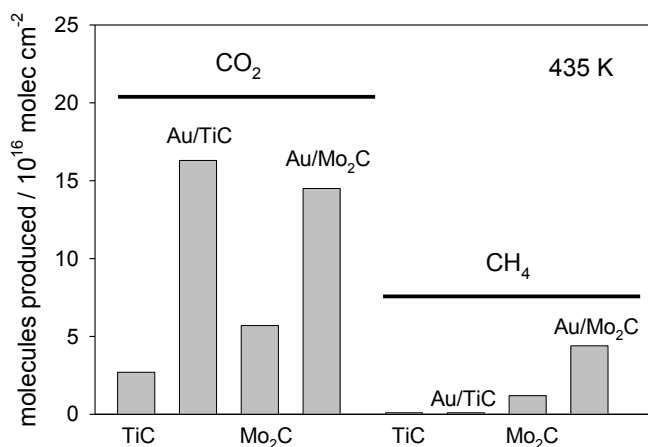


**Figure 4.** Production of CO<sub>2</sub> and CH<sub>4</sub> after exposing TiC(001), Au/TiC(001), Mo<sub>2</sub>C(001) and Au/Mo<sub>2</sub>C(001) catalysts to a mixture of 20 Torr of CO, 10 Torr of H<sub>2</sub>O and 100 Torr of H<sub>2</sub> at 435 K for 5 minutes..

reaction. In general terms, Mo<sub>2</sub>C(001) is more active than TiC(001) for the conversion of CO, but the molybdenum carbide produces a significant amount of methane. The addition of Au to Mo<sub>2</sub>C(001) produces an excellent catalyst for the conversion of CO at low temperature, but it increases simultaneously the production of CO<sub>2</sub>/H<sub>2</sub> and methane. In Figure 4, Au/TiC(001) is the best WGS catalyst in terms of activity and selectivity. The 1:1 metal-to-carbon ratio in TiC(001) makes very difficult the cleavage of the C–O bond in carbon monoxide.<sup>[9,13]</sup> This 1:1 metal-to-carbon ratio also makes TiC(001) less sensitive to the presence of water in the reaction feed. After 6 hours of operation we found no signs for deactivation of the Au/TiC(001) catalyst during the WGS (Figure S1 in supporting information). In contrast, the Au/Mo<sub>2</sub>C(001) catalyst lost ~ 30% of its activity during the same period of time (Figure S1). Mo<sub>2</sub>C powders and Mo<sub>2</sub>C(001) decompose the water molecule to form films of oxycarbides.<sup>[14,18]</sup> This deactivation process was negligible on TiC(001) and Au/TiC(001).

DFT calculations were used to study the mechanism of the WGS reaction on Au/TiC(001). Figure 5 compares the calculated reaction profiles for the WGS on clean TiC(001)<sup>[17]</sup> and Au<sub>4</sub>/TiC(001). The corresponding molecular structures for the reaction intermediates and transition states are displayed in Figure 6. Since the maximum of catalytic activity in Figure 1 occurs when the Au/TiC(001) system contains a large fraction of small 2D particles,<sup>[8,19]</sup> we used a Au<sub>4</sub>/TiC(001) model in our DFT calculations. Such a model has been used before in studies for SO<sub>2</sub> decomposition<sup>[19]</sup> and CO<sub>2</sub> activation,<sup>[9]</sup> providing valuable explanations of fundamental phenomena. Our theoretical study indicated that the optimal path for the WGS on Au/TiC(001) follows an associative mechanism in which a HOCO species is formed after reacting CO with an OH group produced by the dissociation of water. The formation of a key HOCO intermediate has also

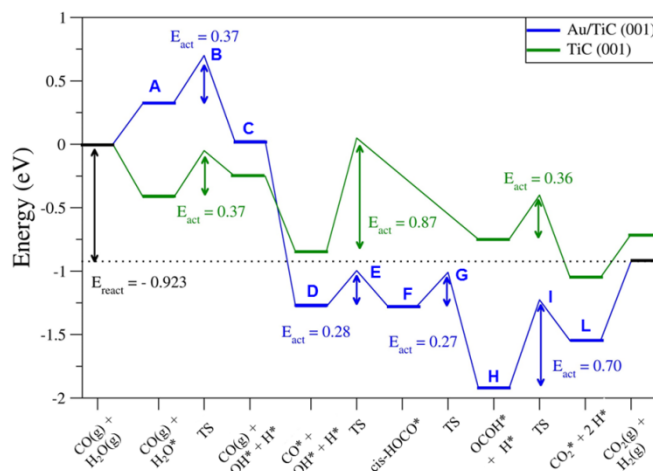


**Figure 5.** DFT calculated energy profile for the WGS reaction on clean TiC(001) and Au<sub>4</sub>/TiC(001). The corresponding molecular structures are shown in Fig. 6.

been proposed in previous theoretical studies for the WGS on Cu(111),<sup>[21]</sup> CeO<sub>x</sub>/Cu(111)<sup>[28]</sup> and Au/TiO<sub>2</sub>(110).<sup>[29]</sup> Table 1 lists the calculated reaction rates for the main steps of the WGS on Au<sub>4</sub>/TiC(001). It is remarkable that on Au<sub>4</sub>/TiC(001) the formation of the HOCO intermediate is an exothermic process that occurs with extremely low activation barriers which are significantly smaller than those found on TiC(001), 0.87 eV,<sup>[17]</sup> or pure gold, > 2eV.<sup>[29]</sup> On clean TiC(001), the calculated reaction rate for the CO + OH → cis-HOCO reaction was only 3.20 s<sup>-1</sup>,<sup>[17]</sup> while on Au<sub>4</sub>/TiC(001) the corresponding rate was 4.14 × 10<sup>8</sup> s<sup>-1</sup>. Surfaces of pure gold do not dissociate water.<sup>[29]</sup> In contrast, the rate for the dissociation of water on a Au<sub>4</sub> cluster supported on TiC(001) is 2.02 × 10<sup>9</sup> s<sup>-1</sup>. Thus, the charge polarization at the Au–TiC interface<sup>[8,25]</sup> drastically enhances the catalytic properties of gold.

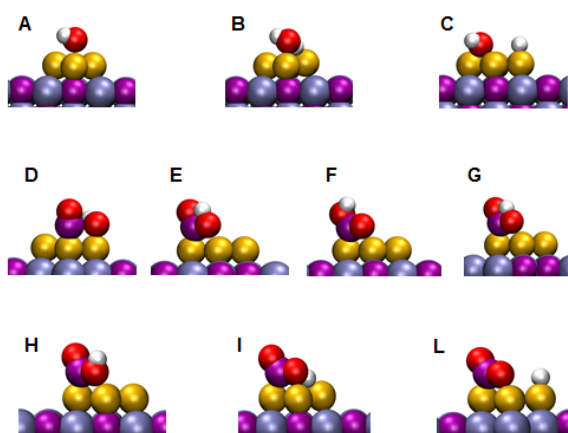


**Figure 6.** Calculated DFT molecular structures for intermediates and TS of the WGS on a Au<sub>4</sub>/TiC(001) model catalyst. The corresponding energy profile is shown in Figure 5. Color code: yellow, Au; purple, C; grey, Ti; red, O; white, H

**Table 1.** Calculated barriers and rates for main steps of the WGS on Au<sub>4</sub>/TiC(001). E<sub>act</sub> is in eV/molecule and reaction rates (RR) in s<sup>-1</sup>.

Reaction	E <sub>act</sub>	RR
H <sub>2</sub> O → OH + H	0.37	2.02 × 10 <sup>9</sup>
CO + OH → cis-HOCO	0.28	4.14 × 10 <sup>8</sup>
cis-HOCO → trans-OCOH	0.27	1.29 × 10 <sup>10</sup>
OCOH → CO <sub>2</sub> + H	0.70	2.30 × 10 <sup>3</sup>

A detailed comparison of the behaviour of Au on TiC(001) and TiO<sub>2</sub>(110) or ZnO(000 $\bar{1}$ ) points to strong metal-support interactions on the carbide surface which make this substrate the best option for enhancing the WGS activity of Au. The 1:1 metal-to-carbon ratio in TiC provides stability and prevents the transformation of CO into methane. In Au/TiC(001), one has a highly active and selective catalyst for the low temperature WGS reaction.

## Experimental Section

The Au/TiC(001) and Au/Mo<sub>2</sub>C(001) catalysts were prepared and tested in an ultrahigh vacuum chamber that has attached a high-pressure cell or batch reactor.<sup>[13,27,29]</sup> Au was deposited on the metal carbide substrates following the methodology described in refs. 19 and 25. The procedures followed for the cleaning of the TiC(001) and Mo<sub>2</sub>C(001) surfaces are described elsewhere.<sup>[13,19,25]</sup> In the experiments, the WGS activity of the metal/carbide catalysts was tested under mixtures of CO/H<sub>2</sub>O or CO/H<sub>2</sub>O/H<sub>2</sub>.<sup>[14,26-29]</sup> The CO gas was stored on aluminium tanks and cleaned of any metal carbonyl impurity by passing it through purification traps.

The periodic DFT calculations estimated exchange and correlation energy using the PW91-GGA<sup>[30]</sup> approximation as implemented in VASP.<sup>[31]</sup> The wave function was expanded using a plane wave basis set whose associated kinetic energy was lower than 415 eV. A suitable net of 3×3×1 **k** points generated using Monkhorst-Pack algorithm was used to perform integration in the reciprocal space.<sup>[32]</sup> The Au<sub>4</sub> cluster was adsorbed on a 3(√2×√2)R45° supercell and fully relaxed together with all adsorbates and the two upper layers of the slab until forces were smaller than 0.02 eV Å<sup>-1</sup>. About 10 Å of vacuum perpendicular to the surface avoided interaction between repeated images. Transition states were identified using CI-NEB algorithm.<sup>[33]</sup> All structures were characterised as proper minima or saddle points by vibrational analysis. Reaction rates were estimated from standard transition state theory including the calculation of the vibrational partition function as detailed elsewhere.<sup>[17]</sup>

**Keywords:** Metal-support interactions • Gold activation • Titanium carbide • Hydrogen production • Low-temperature water-gas shift reaction

- [1] C.T. Campbell, *Nature Chemistry*, **2012**, *4*, 597-598.
- [2] S.J. Tauster, *Accounts of Chem. Research*, **1987**, *20*, 389-394.
- [3] A.K. Datye, D.S. Kalakkad, M.H. Yao, D.J. Smith, *J. Catal.* **1995**, *155*, 148-153.
- [4] A. Bruix, J.A. Rodriguez, P.J. Ramirez, S.D. Senanayake, J. Evans, J.B. Park, D. Stacchiola, P. Liu, J. Hrbek, F. Illas, *J. Am. Chem. Soc.* **2012**, *134*, 8968-8974.
- [5] S.D. Senanayake, J.A. Rodriguez, D. Stacchiola, *Topics in Catal.* **2013**, *56*, 1488-1498.
- [6] N.M. Schweitzer, J.A. Schaidle, O.K. Ezekoye, X. Pan, S. Linic, L.T. Thompson, *J. Am. Chem. Soc.* **2011**, *133*, 2378-2381.
- [7] L.K. Ono, B. Roldán-Cuenya, *Catal. Lett.* **2007**, *113*, 86-94.
- [8] J.A. Rodriguez, F. Illas, *Phys. Chem. Chem. Phys.* **2012**, *14*, 427-438
- [9] A. Vidal, L. Feria, J. Evans, Y. Takahashi, P. Liu, K. Nakamura, F. Illas, J.A. Rodriguez, *J. Phys. Chem. Lett.* **2012**, *3*, 2275-2280.
- [10] M.D. Porosoff, X. Yang, J.A. Boscoboinik, J.G. Chen. *Angew. Chem. Int. Ed.* **2014**, *53*, 1-6.
- [11] J.G. Chen, *Chem. Rev.* **1996**, *96*, 1477-1498.
- [12] S.T. Oyama, *Catal. Today*, **1992**, *15*, 179-200.
- [13] S. Posada-Pérez, F. Viñes, P.J. Ramirez, A.B. Vidal, J.A. Rodriguez, F. Illas, *Phys. Chem. Chem. Phys.*, **2014**, in press, DOI:10.1039/c4cp01943a.
- [14] D.J. Moon, J. W. Ryu, *Catal. Lett.* **2004**, *92*, 17-24.
- [15] P.M. Patterson, T.K. Das, B.H. Davis, *Applied Catal. A: General*, **2003**, *251*, 449-455.
- [16] W. Xu, P.J. Ramirez, D. Stacchiola, J.A. Rodriguez, *Catal. Lett.* 2014, in press, DOI: 10.1007/s10562-014-1278-5
- [17] F. Viñes, P. Liu, J.A. Rodriguez, F. Illas, *J. Catal.* **2008**, *260*, 103-112.
- [18] P. Liu, J.A. Rodriguez, *J. Phys. Chem. B*, **2006**, *110*, 19418-19425.
- [19] J.A. Rodriguez, P. Liu, F. Viñes, F. Illas, Y. Takahashi, K. Nakamura, *Angew. Chem. Int. Ed.* **2008**, *47*, 6685-6689.
- [20] R.B. Burch, *Phys. Chem. Chem. Phys.* **2006**, *8*, 5483-5500.
- [21] A.A. Gokhale, J. Dumesic, M. Mavrikakis, *J. Am. Chem. Soc.* **2008**, *130*, 1402-1414.
- [22] K.-Z. Qi, G.-C. Wang, W.-J. Zheng, *Surf. Sci.* **2013**, *614*, 53-63.
- [23] J.-L. Dubois, K. Sayama, H. Arakawa, *Chem. Lett.* **1992**, 5-8.
- [24] J. Nakamura, J.M. Campbell, C.T. Campbell, *J. Chem. Soc., Faraday Trans.* **1990**, *86*, 2725-2734.
- [25] J.A. Rodriguez, P. Liu, F. Viñes, F. Illas, Y. Takahashi, K. Nakamura, *J. Chem. Phys.* **2007**, *127*, 211102.
- [26] R. Si, J. Tao, J. Evans, J.-B. Park, L. Barrio, J.C. Hanson, Y. Zhu, J. Hrbek, J.A. Rodriguez, *J. Phys. Chem. C*, **2012**, *116*, 23547-23555.
- [27] J.A. Rodriguez, P. Liu, J. Hrbek, J. Evans, M. Perez, *Angew. Chem. Int. Ed.*, **2007**, *46*, 1329-1332.
- [28] K. Mudiyansele, S.D. Senanayake, L. Feria, S. Kundu, A.E. Baber, J. Graciani, A.B. Vidal, S. Agnoli, J. Evans, R. Chang, S. Axnanda, Z. Liu, J.F. Sanz, P. Liu, J.A. Rodriguez, D.J. Stacchiola, *Angew. Chem. Intl. Ed.* **2013**, *52*, 5101-5105.
- [29] J.A. Rodriguez, J. Evans, J. Graciani, J.-B. Park, P. Liu, J. Hrbek, J.F. Sanz, *J. Phys. Chem. C*, **2009**, *113*, 7364-7370.
- [30] Y. Wang, J. P. Perdew, *Phys. Rev. B*, **1991**, *43*, 8911-8916.
- [31] G. Kresse, J. Furthmüller, *Comput. Mater. Sci.*, **1996**, *6*, 15-50.
- [32] H.J. Monkhorst, J.D. Pack, *Phys. Rev. B*, **1976**, *13*, 5188-5192.
- [33] G. Henkelman, B.P. Uberuaga, H. Jónsson, *J. Chem. Phys.*, **2000**, *113*, 9901-9904.

**Entry for the Table of Contents** (Please choose one layout)

Layout 1:

**COMMUNICATION**

Text for Table of Contents

((Insert TOC Graphic here))

*Author(s), Corresponding Author(s)\****Page No. – Page No.****Title**

Layout 2:

**COMMUNICATION**

((Insert TOC Graphic here))

*Author(s), Corresponding Author(s)\****Page No. – Page No.****Title**

Text for Table of Contents